

# Identification of a Noncanonically Transcribed Subgenomic mRNA of Infectious Bronchitis Virus and Other Gammacoronaviruses

Kirsten Bentley, Sarah May Keep, Maria Armesto, Paul Britton

Avian Viral Diseases, The Pirbright Institute, Compton Laboratory, Compton, Newbury, Berkshire, United Kingdom

**Coronavirus subgenomic mRNA (sgmRNA) synthesis occurs via a process of discontinuous transcription involving transcription regulatory sequences (TRSs) located in the 5' leader sequence (TRS-L) and upstream of each structural and group-specific gene (TRS-B). Several gammacoronaviruses including infectious bronchitis virus (IBV) contain a putative open reading frame (ORF), localized between the M gene and gene 5, which is controversial due to the perceived absence of a TRS. We have studied the transcription of a novel sgmRNA associated with this potential ORF and found it to be transcribed via a previously unidentified noncanonical TRS-B. Using an IBV reverse genetics system, we demonstrated that the template-switching event during intergenic region (IR) sgmRNA synthesis occurs at the 5' end of the noncanonical TRS-B and recombines between nucleotides 5 and 6 of the 8-nucleotide consensus TRS-L. Introduction of a complete TRS-B showed that higher transcription levels are achieved by increasing the number of nucleotide matches between TRS-L and TRS-B. Translation of a protein from the sgmRNA was demonstrated using enhanced green fluorescent protein, suggesting the translation of a fifth, novel, group-specific protein for IBV. This study has resolved an issue concerning the number of ORFs expressed by members of the *Gammacoronavirus* genus and proposes the existence of a fifth IBV accessory protein. We confirmed previous reports that coronaviruses can produce sgmRNAs from noncanonical TRS-Bs, which may expand their repertoire of proteins. We also demonstrated that noncanonical TRS-Bs may provide a mechanism by which coronaviruses can control protein expression levels by reducing sgmRNA synthesis.**

The *Gammacoronavirus* infectious bronchitis virus (IBV) is an enveloped positive-sense, single-stranded RNA virus that is the etiological agent of the acute highly contagious poultry disease infectious bronchitis (IB) (1–4). Infectious bronchitis virus is a highly infectious pathogen of domestic fowl that replicates primarily in epithelial cells of the respiratory tract causing IB and is responsible for major economic losses to poultry industries worldwide as a result of poor weight gain and decreased egg production (5, 6). In addition, some isolates have been found to be associated with renal disease and can be highly nephropathogenic (7–9).

The IBV genome is typical of other coronaviruses with gene 1, the replicase gene, located at the 5' end of the genome and the structural and group-specific accessory genes clustered at the 3' end. Additionally, for IBV and the closely related gammacoronavirus turkey coronavirus (TCoV), there is a region located between the membrane (M) gene and the group-specific gene 5 referred to as the intergenic region (IR), also known as open reading frame (ORF) 4b or ORF X (10–13). With the exception of the laboratory-adapted attenuated IBV Beaudette strain and some IBV vaccine isolates which contain deletions in this region, the IR contains a putative ORF with the potential to code for a protein of 94 amino acids with a predicted molecular mass of 11 kDa. For both IBV and TCoV there has been speculation over the function of the IR-associated ORF due to the lack of identification of an associated transcription regulatory sequence (TRS) for the generation of a subgenomic mRNA (sgmRNA) for expression of the 11-kDa protein.

The model of coronavirus transcription proposed by Sawicki and Sawicki (14) has led to the general acceptance that transcription of the structural and group-specific genes of coronaviruses occurs via a process of discontinuous transcription during negative-strand synthesis (reviewed in references 15 to 17). A conserved sequence known as the TRS is located at the distal end of

the leader sequence (TRS-L) present at the very 5' end of a coronavirus genome and upstream of each of the structural or group-specific genes (TRS-B). During synthesis of the sgmRNAs, the TRS-B acts a signal for pausing the replication transcription complex. The TRS-B of the nascent negative-strand sgRNA is then able to complementarily base pair with the TRS-L of the genome, facilitating a template switch, and transcription continues to the 5' end of the genome. The negative-sense sgRNAs, with coterminal 5' and 3' ends, are then transcribed into a nested set of positive-sense sgmRNAs from which generally the 5'-most ORF is translated. Evidence for the model of discontinuous transcription during negative-strand synthesis came, in part, from evidence suggesting that the TRS of each sgmRNA was derived from the TRS-B and not the TRS-L (18–20). The precise mechanisms of sgRNA synthesis are, as yet, not fully understood although a number of sequence elements, including the 5' and 3' flanking nucleotides of the TRS, have been identified that may have important roles (18, 20–26).

Identification of TRSs for IBV and TCoV strains is based on the proposed consensus sequence CUUAACAA although some variation in this sequence is seen; for example, the TRS-B of the IBV spike (S) and gene 3 is CUGAACAA. A canonical TRS closely matching this consensus sequence has not been identified upstream of the IBV or TCoV IR, resulting in the belief that no sgmRNA is transcribed and that this region is therefore likely to be a pseudogene. Northern blot analysis of the IBV mRNA profile

Received 22 October 2012 Accepted 27 November 2012

Published ahead of print 5 December 2012

Address correspondence to Paul Britton, paul.britton@pirbright.ac.uk.

Copyright © 2013, American Society for Microbiology. All Rights Reserved.

doi:10.1128/JVI.02967-12

variably identifies the presence of a low-abundance RNA located between the sgRNAs representing the M gene and gene 5. Despite the correlation of the presence of this RNA with the location of the IR, this RNA was originally classified as an unknown species (27) and has been rarely mentioned in the literature since.

In this study, we used an IBV reverse genetics system (28–30) to produce a number of recombinant IBVs (rIBVs) to investigate the IR and confirmed the nature of the low-abundance RNA as an IBV sgRNA from which an IR-associated ORF could be expressed. This study details the use of a noncanonical TRS-B in transcription of this sgRNA and proposes the presence of a fifth novel group-specific protein for IBV and other closely related gamma-coronaviruses. Our study supports previous observations that coronaviruses are able to control the levels of sgRNA expression. These findings offer the possibility that coronaviruses may produce other sgRNAs utilizing similar noncanonical TRS-Bs, consequently increasing the repertoire of accessory genes and providing a potential mechanism by which this important group of viruses is able to control the expression of virus-derived proteins.

## MATERIALS AND METHODS

**Cells and viruses.** Primary chicken kidney (CK) cells were prepared from 2- to 3-week-old specific-pathogen-free (SPF) Rhode Island Red chickens. IBV Beau-R, Beau-CK, and all recombinant viruses were propagated and titrated on primary CK cells using BES [*N,N*-bis(2-hydroxyethyl)-2-aminoethanesulphonic acid] cell maintenance medium (30). Extracellular virus was harvested 24 h postinfection (hpi) and titrated by plaque assay. IBV strains M41, CR88, D1466, H120, Italy-02, and QX were propagated in 10-day-old SPF Rhode Island Red embryonated hens' eggs. Allantoic fluid was harvested at 24 h postinoculation and clarified by low-speed centrifugation.

**Construction of modified IBV cDNA plasmids.** To delete the Beaudette IR, the IBV Beau-R genome corresponding to the region of ORF 3c to the N gene was inserted into pGPTNEB193. The IR sequence, nucleotides (nt) 25192 to 25459 inclusive, was digested out using introduced restriction sites *Nhe*I and *Kpn*I, and an adapter of *Nhe*I-*Sma*I-*Eco*RV-*Mlu*I-*Kpn*I was inserted. The modified region, which maintained the first three amino acids of the putative coding sequence as well as any potential unmodified upstream TRSs, was subcloned into pGPTNEB193 to yield pGPT-BeauRΔIR.

To modify the Beau-R TRS-L for generation of rIBVs BeauR-L-CTG ACAA and BeauR-L-CTTAACAT, the first 500 bp of the Beau-R genome along with the preceding 550 bp of recombinant vaccinia virus (rVV) sequence was amplified by PCR from rVV-Beau-R/T7 and ligated into *Pac*I- and *Hind*III-digested pGPTNEB193 to yield plasmid pGPT-rVV/IBV. The 550-bp vaccinia virus sequence also contained the T7 promoter sequence immediately upstream of the 5' end of the Beau-R genome. To introduce mutations into the TRS-L of pGPT-rVV/IBV, the forward primer BeauR-L-CTGAACAA (5'-TAGATTTTAACTGAAC AAAACGGA-3') or BeauR-L-CTTAACAT (5'-TAGATTTTAACTTAA CATAACGGAC-3') was used together with the reverse primer BeauR-L-CTGAACAA (5'-GTCCGTTTGTTCAGTTAAAAATCTA-3') or BeauR-L-CTTAACAT (5'-GTCCGTTATGTTAAGTAAAAATCTA-3') to generate plasmids pGPT-L-CTGAACAA and pGPT-L-CTTAACAT.

Plasmids pGPT-eGFPΔ4b and pGPT-IR-CTGAACAA, used to generate rIBVs BeauR-eGFPΔ4b and BeauR-IR-CTGAACAA, respectively, were generated by GeneArt. Gene synthesis was carried out to incorporate either enhanced green fluorescent protein (eGFP) or mutations <sup>2507</sup>G → C and <sup>2507</sup>C → A into the region of Beau-R corresponding to the M gene to ORF 5a, followed by cloning of the synthesized genome segments into pGPTNEB193.

**Generation of recombinant vaccinia viruses containing modified IBV cDNA and recovery of infectious IBV.** Modified regions of IBV cDNA within plasmids pGPT-BeauRΔIR, pGPT-L-CTGAACAA, pGPT-

L-CTTAACAT, pGPT-eGFPΔ4b, and pGPT-IR-CTGAACAA were introduced into the IBV Beaudette full-length cDNA within the vaccinia virus genome by homologous recombination using transient dominant selection, as described previously (29, 30). Infectious rIBVs were recovered from recombinant vaccinia viruses containing the correctly modified IBV cDNAs and passaged three times on CK cells prior to experimental use.

**Leader-body junction analysis.** Intracellular RNA was reverse transcribed using SuperScript III (Invitrogen) with the random primer 5'-GTTTCCCAGTCACGATCNNNNNNNNNNNNNNNNNN-3'. Resulting cDNAs were amplified by PCR with a forward primer located within the 5' leader sequence (for IBV, 5'-CTATTACTAGCCTTGCGC-3'; for TCov, 5'-CTATCATACTAGCCTTGTC-3') and the reverse primer 5'-GACCACATCCTACAACAACC-3' located within the IR sequence. Templates were denatured at 94°C for 2 min, followed by 25 cycles of 94°C for 30 s, 50°C for 30 s, and 72°C for 30 s. PCR products were cloned using a TOPO TA Cloning Kit for Sequencing (Life Technologies).

**Northern blot analysis.** Intracellular RNA was extracted from CK cells at 24 hpi using an RNeasy Mini Kit following the protocol for animal cells (Qiagen) with homogenization using a TissueLyser II for 30 s at 25 Hz (Qiagen). mRNA was purified using a Poly(A)Purist MAG Kit (Ambion), as per the manufacturer's instructions. Northern blot analysis was carried out with a NorthernMax-Gly Kit (Ambion). Briefly, viral mRNA transcripts were denatured in glyoxal loading dye at 50°C for 30 min, followed by separation on a 0.8% low-electroendosmosis (LE) agarose gel. RNA was transferred to BrightStar-Plus positively charged nylon membrane (Ambion) using capillary action for 2 h, cross-linked by treatment with UV light using the auto-cross-link function on a Stratilinker UV Cross-linker (Stratagene), and prehybridized for 30 min with ULTRAhyb buffer at 42°C. Blots were probed with a cDNA probe specific to the 3' end of IBV [forward primer, 5'-CAACAGCGCCCAAAGAAG-3', within the N gene; reverse primer, 5'-GCTCTAACTCTATACTAGCCT-3', directly preceding the poly(A) tail] and labeled using a BrightStar Psoralen-Biotin Non-isotopic Labeling Kit (Ambion). Blots were hybridized overnight at 42°C, followed by washing and development with a BrightStar BioDetect Kit.

**Growth kinetics of rIBVs.** Individual wells of six-well plates of confluent CK cells were infected with  $1 \times 10^5$  PFU of virus and incubated for 1 h at 37°C in 5% CO<sub>2</sub>, after which cells were washed twice with phosphate-buffered saline (PBS), and 2 ml of fresh 1× BES medium was added. Extracellular virus was harvested at 1, 8, 12, 24, 48, and 72 h and subsequently analyzed in triplicate by plaque assay on CK cells for progeny virus.

**IR protein identification.** Antibody generation was carried out by Cambridge Research Biochemicals (United Kingdom). Briefly, a synthetic peptide corresponding to amino acids 68 to 84 (DNGKVYEGKPIQ KGC) of the IBV M41 IR protein was synthesized and used to immunize two rabbits. Crude antisera were pooled and purified by affinity chromatography on thiopropyl-Sepharose 6B coupled with antigen. Samples of M41-infected CK cell lysates were separated on 10% bis-Tris precast polyacrylamide gels (Life Technologies). Separated proteins were transferred to nitrocellulose membrane (Amersham Hybond ECL) and probed with the purified IR antibody. Potentially bound antibody was visualized using an enhanced-chemiluminescence detection system (ECL) (Millipore).

**Real-time PCR.** RNA was harvested from CK cells at 24 hpi as described previously and reverse transcribed using 0.5 μg of RNA per reaction. The following cDNAs were synthesized at 48°C for 0.5 h followed by inactivation of the reverse transcriptase at 95°C for 5 min with TaqMan Reverse Transcription Reagents (ABI) and 2 pmol of reverse primer (for 28S, 5'-GACGACCGATTTGCACGTC-3'; IBV gene 3, 5'-TGGGACTTT GGATCATCAAACA-3'; IBV IR, 5'-GCATAGACAAACGTAGCAAAC CTTT-3'). The synthesized cDNAs were used as templates for specific PCR amplification with the reverse primer as above and a forward primer for 28S (5'-GGGGAAGCCAGAGGAAACT-3') or IBV cDNAs (5'-CTA GCCTTGCGTAGATTTTAACT-3') and a probe for 28S (6-FAM-AG GACCGCTACGACCTCCACCA-TAM) IBV gene 3 (6-FAM-CAATAC AGACCTAAAAAGT-MGB), or IBV IR (6-FAM-ACAAAGCGGAAATA

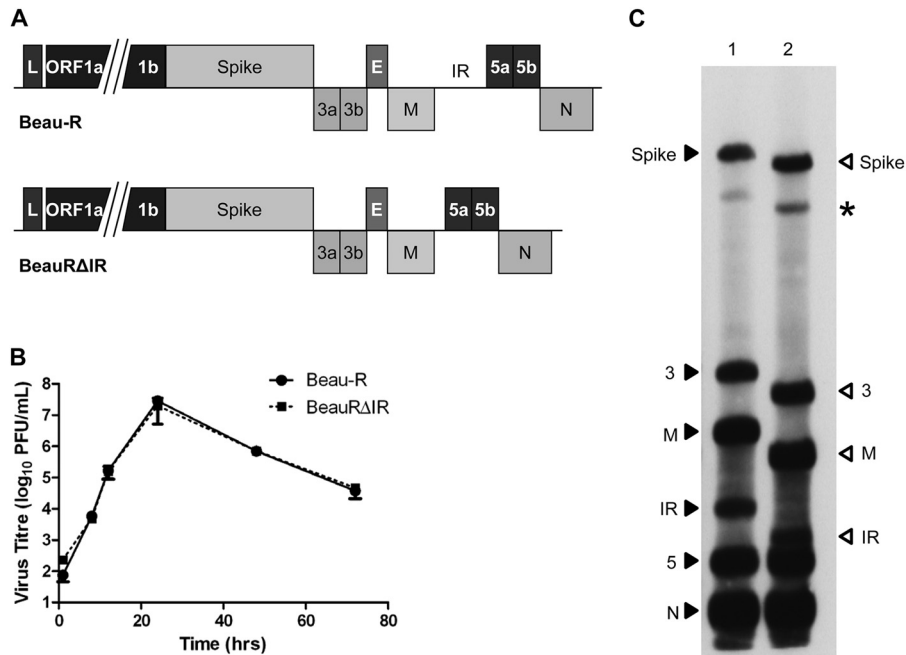


**FIG 1** Characterization of an rIBV with the IR deleted. The IR of Beau-R was deleted, resulting in rIBV Beau- $\Delta$ IR. (A) Schematic diagram showing the genome organizations of Beau-R and Beau- $\Delta$ IR. Beau- $\Delta$ IR contains a 268-nt deletion, downstream of amino acid 3, reducing the IR sequence of Beau-R to 37 nt in length. (B) Growth kinetics of Beau- $\Delta$ IR. Monolayers of CK cells were infected with  $1 \times 10^5$  PFU of Beau-R or Beau- $\Delta$ IR, and extracellular virus was harvested at 1, 8, 12, 24, 48, and 72 h. Virus was titrated in triplicate by plaque assay on CK cells. Error bars represent standard deviations of the mean results from three independent experiments. (C) Northern blot analysis of the sgRNAs produced by Beau- $\Delta$ IR. Lane 1, Beau-R; lane 2, Beau- $\Delta$ IR. The asterisk indicates an additional sgRNA derived from within the S gene. L represents the leader sequence at the 5' end of the IBV genome, E the envelope protein gene, and N the nucleoprotein gene.

A-MGB) (where FAM is 6-carboxyfluorescein, TAM is 6-carboxytetramethylrhodamine, and MGB is minor groove binder). All primers and probes were designed using Primer Express software. Each 10- $\mu$ l real-time PCR mixture consisted of 5  $\mu$ l of TaqMan Fast Universal PCR Master Mix (2 $\times$ ), 0.2  $\mu$ l of a 1  $\mu$ M primer mix, 0.25  $\mu$ l of probe (5  $\mu$ M), 2.05  $\mu$ l of water, and 2.5  $\mu$ l of cDNA. All reactions were performed in triplicate in a 7500FAST TaqMan machine (Applied Biosystems) at 95°C for 20 s, followed by 40 cycles of 95°C for 3 s and 60°C for 30 s. Amplification plots were analyzed using Applied Biosystems Sequence Detection Software, version 1.3.1.21.

## RESULTS

**Identification of an mRNA corresponding to the IBV intergenic region.** Northern blot analysis of the IBV mRNA profile has identified a low-abundance RNA of unknown origin located between the sgRNAs representing the M gene and gene 5. Data obtained while working on a number of rIBVs led to the suggestion of a link between the IR ORF and this low-abundance RNA species. To investigate this association in more depth, we used our IBV reverse genetics system to construct rIBV Beau- $\Delta$ IR, a recombinant virus based on IBV Beau-R, a molecular clone of the Beaudette-CK strain of IBV (28). Recombinant IBV Beau- $\Delta$ IR contains a 268-nt deletion within the IR beginning at amino acid 4 of the putative coding sequence (Fig. 1A). The deleted region did not disrupt sequences required for transcription of upstream and downstream genes and was designed to ensure that any potential upstream regulatory sequences that would be required for transcription of an sgRNA for the IR were maintained. Growth analysis of this virus in primary chicken kidney (CK) cells showed that it displayed kinetics and peak titers equivalent to those of wild-type Beau-R (Fig. 1B). Northern blot analysis of the RNA species pro-

duced by rIBV Beau- $\Delta$ IR showed a reduction in size of the low-abundance RNA species in question and in the other larger sgRNAs, consistent with the size of the deletion introduced into the Beau-R IR, providing a strong indication that this RNA is an sgRNA corresponding to the IR of IBV Beaudette (Fig. 1C).

As no specific TRS has ever been identified upstream of the IR ORF, the question of how this potential sgRNA is transcribed was addressed. Intracellular RNA was extracted from CK cells infected with a variety of field and vaccine strains of IBV, and sgRNAs were amplified by leader-body junction reverse transcription-PCR (RT-PCR), as described previously (28). An sgRNA corresponding to the IR was identified as a PCR product of approximately 400 bp (350 bp for Beau-R and parent virus Beau-CK) (Fig. 2A). Sequence analysis of the RT-PCR products confirmed that each virus produced an sgRNA corresponding to the IR as each RT-PCR product contained the IBV leader sequence followed by the canonical IBV TRS, CUUAACAA, as expected for all sgRNA transcripts (Fig. 2B). However, sequence alignments showed that only positions 6 to 8, CAA, of the IBV TRS and not the entire consensus sequence had perfect homology to the IBV genomic sequence upstream of the IR. This CAA sequence is located approximately 100 nt upstream of the proposed AUG for the IR ORF, a distance consistent with distances observed for the currently known IBV TRS-Bs and associated genes. These results confirmed that all the IBV strains analyzed produce an sgRNA corresponding to the IR and suggested that transcription of this new sgRNA species of IBV is initiated from a noncanonical TRS-B where the consensus 8-nucleotide TRS of CUUAACAA is reduced to CAA.

The presence and sequence of the IR-derived sgRNA were

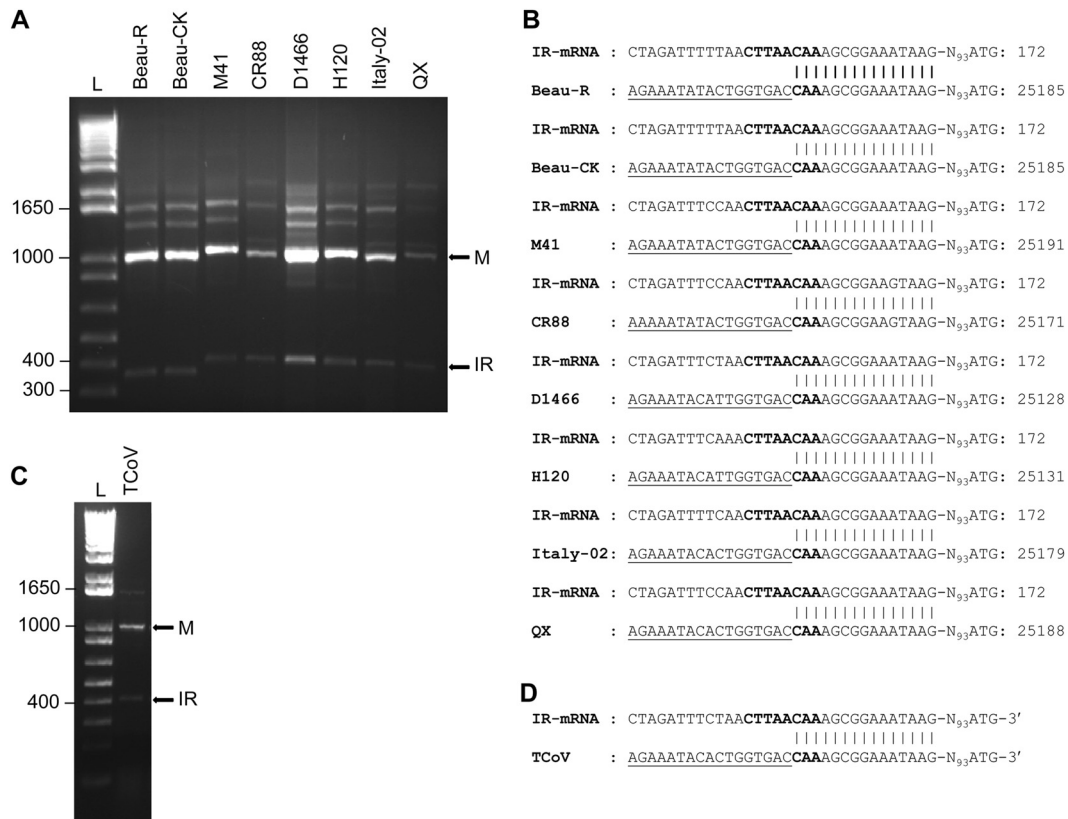


**FIG 2** Analysis of leader-body TRS junctions of IR sgmRNAs of IBV and TCoV isolates. Intracellular RNA was extracted from CK cells 24 hpi with IBV or from turkey embryos inoculated with TCoV strain FR080385d. Virus mRNAs were RT-PCR amplified with primers specific to leader sequence and the IR for both IBV and TCoV. (A and C) Agarose gel electrophoresis of RT-PCR products amplified from IBV or TCoV mRNAs, respectively. Lanes L, molecular size ladder. (B and D) Sequence analysis of the IR mRNA transcripts from IBV-infected CK cells or TCoV-inoculated turkey embryos, respectively. The virus genome sequence is shown below, and the mRNA sequence is shown above. The leader-body TRS junction is marked in bold, the unaligned genome sequence upstream of the leader-body junction is underlined, and the initiation codon ATG of the 11-kDa ORF encoded in the IR is shown at the 3' end. The relative nucleotide position of the ATG from the end of the IR mRNA (top sequence) or from the 5' end of the Beaudette genome (bottom sequence) is given.

also confirmed using RNA extracted from the tracheas of birds experimentally infected with the M41 strain of IBV, thus ruling out the possibility that this sgmRNA is an artifact of cell culture infection (data not shown). Given the identification of the 11-kDa ORF sequence in the closely related gammacoronavirus TCoV, a BLASTn search was carried out on a 50-nt region covering the proposed IBV IR TRS site and was found to have 98% homology with several TCoV sequences (data not shown), suggesting a possible conserved mechanism of transcription. Analysis of RNA extracted from turkey embryos experimentally infected with TCoV strain FR080385d confirmed that an sgmRNA corresponding to the TCoV IR ORF is also transcribed using a similar noncanonical TRS-B to IBV (Fig. 2C and D). Further investigation of available *Gammacoronavirus* genome sequences revealed that viruses isolated from at least three other avian species also contain both the putative coding region and the conserved region of the noncanonical TRS: duck coronavirus (JF705860), partridge coronavirus (AY646283), and pheasant coronavirus ph/UK/602/95 (D. Cavanagh and P. Britton, unpublished data).

**The IBV sgmRNA transcribed via the noncanonical TRS can be translated.** To date, the 11-kDa 94-amino-acid protein sequence encoded by the IR-associated ORF has only been discussed with regard to its potential to be translated due to the lack of proof of an sgmRNA. Confirmation that an IR sgmRNA is produced

during an IBV infection suggested that the IR-associated 11-kDa protein is translated but has yet to be identified. To begin to address this issue, a synthetic peptide corresponding to the IBV M41 IR sequence was generated, and antibodies were raised against this peptide. However, Western blot analysis of IBV M41-infected CK cells proved inconclusive in identifying the 11-kDa protein when cells were probed with this IR antibody.

To strengthen the case for the existence of a fifth accessory protein of IBV, an alternative method utilizing our IBV reverse genetics system was pursued. An rIBV, BeauR-eGFP $\Delta$ 4b, was engineered that replaced the IR ORF with that of enhanced green fluorescent protein (eGFP) so that the AUG of the 11-kDa ORF became the initiation codon for eGFP (Fig. 3A). Following infection of CK cells with rIBV BeauR-eGFP $\Delta$ 4b, fluorescence could be observed in infected cells (Fig. 3B). The eGFP sgmRNA showed the same TRS usage as that of the IR and confirmed that a protein can be translated from this newly confirmed IBV sgmRNA transcribed using the proposed noncanonical TRS-B (Fig. 3C).

**Determination of the origin of the TRS in the IR sgmRNA.** In accordance with the mechanism of coronavirus sgmRNA transcription, we hypothesized that leader-body TRS base pairing for the *de novo* synthesized IR sgmRNA was centered on the CAA sequence of the noncanonical TRS-B and the complementary nucleotides of the TRS-L. This would suggest, therefore, that nu-

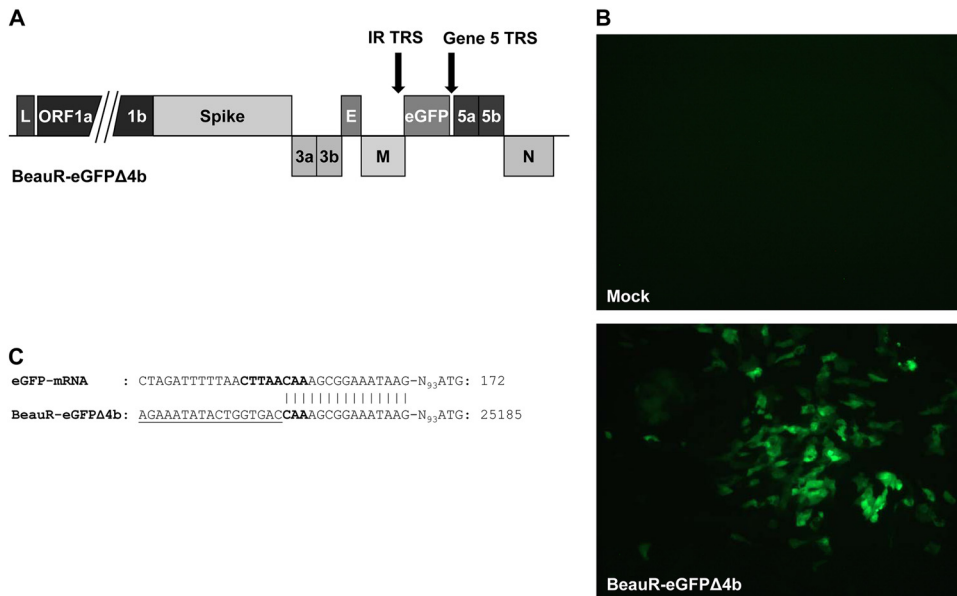


**FIG 3** Translation of eGFP encoded within the IR mRNA. The putative coding region of the Beau-R IR was replaced with eGFP, generating rIBV BeauR-eGFPΔ4b. (A) Schematic diagram of the genome organization of BeauR eGFPΔ4b. (B) Fluorescence microscopy of CK cells infected with BeauR-eGFPΔ4b. Images were taken at 18 hpi at  $\times 10$  magnification. (C) Sequence analysis of the eGFP mRNA transcript expressed by BeauR-eGFPΔ4b in CK cells. The virus genome sequence is shown below, and the mRNA sequence is above. The leader-body TRS junction is in bold, unaligned genome sequence is underlined, and the IR ATG is shown at the 3' end relative to the leader-body junction as in Fig. 2.

cleotide positions 1 to 5 of the sgmRNA TRS are derived from the TRS-L, following a recombination event and template switch between nucleotides 5 and 6 of the CUUAACAA TRS-L. To test this hypothesis, two point mutations were individually engineered into the TRS-L of Beau-R resulting in two rIBVs: (i) BeauR-L-CTGAACAA, which contained a U  $\rightarrow$  G mutation at nucleotide position 3, and (ii) BeauR-L-CTTAACAT, which contained an A  $\rightarrow$  U mutation at nucleotide position 8 of the consensus TRS-L. Both rIBVs replicated efficiently in CK cells, achieving peak titers of  $1.9 \times 10^7$  PFU/ml and  $1.8 \times 10^7$  PFU/ml, respectively, and displayed similar growth kinetics as observed for wild-type Beau-R (Fig. 4A).

The sequences of the leader-body TRS junctions of the IR sgmRNAs produced by the two rIBVs were investigated as described previously. Sequence analysis showed that the TRS of the IR sgmRNA produced by rIBV BeauR-L-CTTAACAT was CUUAACAA, the same as for Beau-R. This result confirmed that nucleotides 6 to 8, CAA, of the sgmRNA TRS are derived from the truncated TRS-B associated with the generation of an sgmRNA for the IR. However, the TRS of the IR sgmRNA produced by rIBV BeauR-L-CTGAACAA showed incorporation of the U  $\rightarrow$  G mutation at nucleotide position 3, demonstrating the involvement of nucleotides 1 to 5 from the TRS-L in forming the TRS of the IR sgmRNA (Fig. 4B). The incorporation of the nucleotide change at position 3, but not at position 8, is consistent with our hypothesis that the template switch during synthesis of the IR sgmRNA occurs upstream of the truncated CAA TRS-B and suggests a recombination point between nucleotides 5 and 6 of the conserved CUUAACAA TRS-L, a finding that demonstrates that in this case the full-length, 8-nucleotide TRS-B of IBV is not required to initiate template switching.

**The noncanonical TRS-B is responsible for reduced sgmRNA levels.** Northern blot analysis of the RNA species produced by

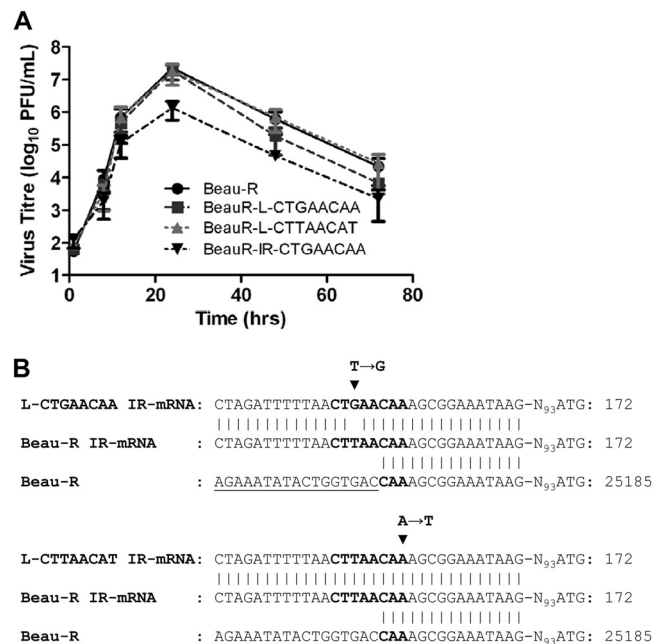


**FIG 4** Characterization of rIBVs containing point mutations within the TRS-L or TRS-B of Beau-R. (A) Growth kinetics of the rIBVs. Monolayers of CK cells were infected with  $1 \times 10^5$  PFU of each virus, and extracellular virus was harvested at 1, 8, 12, 24, 48, and 72 h. Virus was titrated in triplicate by plaque assay on CK cells. Error bars represent standard deviations of the mean results from three independent experiments. (B) Sequence analysis of the IR mRNA transcripts expressed in CK cells infected with rIBVs BeauR-L-CTGAACAA or BeauR-L-CTTAACAT. The virus genome sequence is shown at the bottom, the sequence of the IR mRNA from Beau-R is shown in the middle, and the sequences of the IR mRNAs from the rIBVs are shown at the top. Leader-body TRS junctions are in bold, unaligned genome sequence is underlined, and the IR ATG is shown at the 3' end relative to the leader-body junction as in Fig. 2. Arrows indicate sites of point mutations in the Beau-R TRS-L.

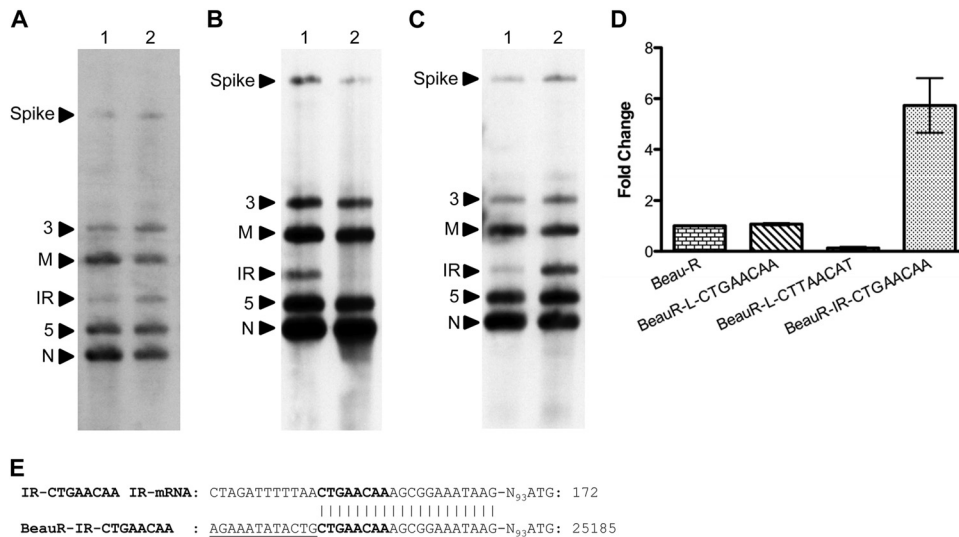


**FIG 5** Analysis of IR sgmRNA levels expressed in rIBVs with TRS mutations. Intracellular RNA was harvested from CK cells at 24 hpi. (A, B, and C) Northern blot analysis of the mRNAs expressed by the rIBVs. Lanes 1, Beau-R; lanes 2, rIBV BeauR-L-CTGAACAA, BeauR-L-CTTAACAT, or BeauR-IR-CTGAACAA, respectively. (D) Quantification of the IR mRNA levels by qRT-PCR using 28S expression as an internal standard. Values were additionally normalized to gene 3 sgmRNA levels to account for variations in infection and replication rates. Error bars represent the standard deviations of the means of two independent experiments. (E) Sequence analysis of the BeauR-IR-CTGAACAA IR mRNA transcript expressed in CK cells. The virus genome sequence is shown below, the mRNA sequence is shown above. The leader-body TRS junction is in bold, unaligned genome sequence is underlined, and the IR ATG is shown at the 3' end relative to the leader-body junction as in Fig. 2.

rIBVs with a modified TRS-L showed, in comparison to Beau-R, a reduction in the IR sgmRNA level from rIBV BeauR-L-CTTAACAT but not from rIBV BeauR-L-CTGAACAA (Fig. 5A and B). This is consistent with previous reports for other coronaviruses describing the disruption of leader-body TRS junctions of group-specific genes (31). Given the reduced level of the IR sgmRNA observed from rIBV BeauR-L-CTTAACAT and the low and variable levels observed from Beau-R, we hypothesized that introduction of a complete consensus TRS-B would increase the hybridization efficiency between TRS-B and TRS-L, resulting in an increase in the amount of IR sgmRNA produced. To test this hypothesis, two point mutations were engineered into the Beau-R genome, <sup>25070</sup>G → C and <sup>25074</sup>C → A, resulting in an IR TRS-B with the sequence CUGAACAA, equivalent to the TRS-B for the S gene and gene 3 of IBV Beaudette (Table 1). A TRS-B with the sequence CUGAACAA was adopted because the introduction of a modified TRS-B with the consensus sequence CUUAACAA

**TABLE 1** Sequence context of the TRS-B sequences in the IBV Beaudette genome

IBV sgmRNA	Sequence <sup>a</sup>
Leader	TTAA <b>CTTAACAA</b> ACGGAC
S	AAA <b>ACTGAACAA</b> AAGACAG
Gene 3	GTA <b>ACTGAACAA</b> TACAGAC
M	AAA <b>CTTAACAA</b> TCCGGAA
IR	ACTGGTGAC <b>CAA</b> AGCGGAA
Gene 5	AAA <b>CTTAACAA</b> ATACGGA
N	CTTT <b>CTTAACAA</b> AGCAGGA

<sup>a</sup> The consensus TRS is highlighted in bold. The flanking nucleotides, both 5' and 3' of the consensus TRS for generating each sgmRNA, are presented to show the nucleotides 5' and 3' of the TRS that may hybridize with the corresponding flanking nucleotides of the TRS-L. Nucleotides 3' to the IR TRS-B showing homology to TRS-L flanking nucleotides are underlined.

would have resulted in a premature stop within the essential M gene. The introduction of these nucleotide changes gave rise to two amino acid changes, G189A and D190E, respectively, within the M protein. An rIBV, BeauR-IR-CTGAACAA, containing the two mutations was produced, and sequence analysis confirmed that the TRS-B for generating the sgmRNA was modified as expected (data not shown).

The growth kinetics of rIBV BeauR-IR-CTGAACAA were found to be similar to that of Beau-R although peak titers at 24 h were approximately 1 log<sub>10</sub> lower (Fig. 4A), likely due to the amino acid changes within the M protein. Northern blot analysis of the RNA species produced by rIBV BeauR-IR-CTGAACAA demonstrated an observable increase in the amount of the IR sgmRNA to a level more comparable with upstream and downstream sgmRNA levels (Fig. 5C), with no apparent effect on the larger sgmRNA species. These results were paralleled by quantitative RT-PCR (qRT-PCR) analysis, which showed a 6-fold increase in the amount of the IR sgmRNA from rIBV BeauR-IR-CTGAACAA and a 0.1-fold change in the amount of the IR sgmRNA from rIBV BeauR-L-CTTAACAT compared to levels from Beau-R (Fig. 5D). As with Northern blot analysis (Fig. 5A), no change in IR level was observed for rIBV BeauR-L-CTGAACAA. This result was expected based on the previous finding that nucleotides 1 to 5 of the TRS-L are not involved in hybridization with the IR TRS-B, and thus alterations to this sequence will not influence hybridization efficiency and, therefore, subsequent sgmRNA levels.

Leader-body junction RT-PCR analysis of the IR sgmRNA from rIBV BeauR-IR-CTGAACAA confirmed the sequence of the leader-body junction TRS as CUGAACAA (Fig. 5E), indicating that the IR sgmRNA TRS was now wholly derived from the modified, near-consensus TRS-B, as predicted by the model of coronavirus sgmRNA synthesis. The stability of the modifications to the IR TRS was investigated by serial passage of rIBV BeauR-IR-

CTGAACAA on CK cells. The modified IR TRS-B sequence was found to be maintained within the Beau-R genome for up to at least eight passages. As has also been observed by others (20, 31), these results demonstrated not only that the TRS-B naturally regulates sgRNA levels but also that stable modifications can be made to the TRS-B that alter the level of transcription of the associated gene.

## DISCUSSION

This work has for the first time identified and confirmed that an RNA species previously observed at low levels in IBV-infected cells and with no known origin is an IBV sgRNA. This sgRNA is capable of expressing an uncharacterized ORF identified in IBV (10), as well as in other closely related gammacoronaviruses such as TCoV (11, 13). Coronaviruses possess the largest RNA genomes, sharing a similar gene order in which genes encoding structural and group-specific accessory proteins are clustered at the 3' end of the genome. Together with the related arteriviruses, coronaviruses have evolved a distinct mechanism for expression of the structural and accessory proteins involving translation from a 3' and 5' coterminal nested set of sgRNAs. These sgRNAs are copied from a series of negative-sense RNA templates synthesized from the genomic RNA by a mechanism involving a discontinuous step that adds the common 5' leader sequence, derived from the 5' end of the genomic RNA, to each sgRNA (14, 16, 32). It has previously been shown that an important factor regulating the process of generating negative-sense RNA templates is the TRS (18–20, 25, 33). A TRS consists of a short AU-rich sequence located at both the 5' leader sequence (TRS-L) and upstream of each structural or group-specific gene (TRS-B) and is known to facilitate the template switch required to complete the synthesis of each negative-sense copy of an sgRNA.

In studying the origin of a potential sgRNA for the translation of the IR ORF of IBV and TCoV (also called ORF 4b or ORF X), we have identified the existence of a naturally occurring sgRNA for a coronavirus that contains a consensus TRS derived predominantly from the TRS-L (Fig. 4B), indicating that the template switch has occurred at a position within the conserved sequence of the TRS-L. The TRS-B for the IR sgRNA was found to consist of only three nucleotides, CAA, corresponding to positions 6 to 8 of the highly conserved IBV CUUAACAA TRS, a finding that begins to explain the previous lack of identification of a TRS-B associated with the IR ORF and the resulting uncertainty over the function of this genome region (Fig. 2B and D). We have demonstrated that the newly confirmed IBV IR sgRNA was generated using an identical noncanonical TRS-B for a variety of vaccine and field isolates of IBV and was also detected in tracheal cells isolated from IBV-infected chickens. Complete genome sequencing of the closely related gammacoronavirus TCoV had revealed the presence of a sequence resembling the IBV IR for which the authors suggested a potential TRS-B, GUCAACAA, located 288 nt upstream of the initiation codon (13). We have demonstrated, using TCoV RNA isolated from infected turkey embryos, that an IR sgRNA is produced from an identical position to that identified in IBV, approximately 100 nt upstream of the initiation codon and utilizing a TRS-B of CAA as identified for IBV.

Although the synthesis of sgRNAs from noncanonical TRSs has been reported previously (34, 35), in this case the noncanonical TRS is a truncation of the consensus CUUAACAA TRS, and the leader-body fusion site contains the canonical TRS, CUUAA

CAA, as expected based on other IBV sgRNAs. The introduction of point mutations into the TRS-L demonstrated that nucleotides 1 to 5 of the leader-body fusion site were derived from the TRS-L, with nucleotides 6 to 8 derived from the TRS-B, indicating that the template switch for the IR sgRNA was occurring upstream of the noncanonical CAA TRS-B and between nucleotides 5 and 6 of the TRS-L. Although the mechanisms for controlling the template switching event during coronavirus and arterivirus discontinuous transcription are not yet fully understood, there is increasing evidence for the requirement of additional sequence elements that in some way control the process, whether by acting at the sequence level or through formation of specific RNA structures (20–24, 26, 36), as well as the potential for RNA-protein interactions (17, 37–40). In particular the 5' and 3' sequences flanking the TRS have been shown to be important, with previous reports for transmissible gastroenteritis virus (TGEV) demonstrating that the four nucleotides either side of the core sequence of CUAAAC were important for predicting mRNAs at noncanonical junction sites (25, 26).

As the sequence of the IR sgRNA noncanonical TRS, CAA, occurs approximately 280 times throughout the Beau-R genome without generating sgRNAs, it is likely that flanking sequences have an important role to play in initiating recognition of the IR TRS-B and the subsequent template switch. Analysis of the Beau-R genome shows regions of homology, both 5' and 3' to the noncanonical TRS-B, with the TRS-L and flanking sequences (Table 1); specifically, 5 of 7 of the IR 3' flanking nucleotides (Table 1, underlined) are complementary to the leader sequence and are likely involved in establishing this sequence as a site for a template switch and sgRNA synthesis.

We have demonstrated, by producing rIBVs with specific modifications to either the TRS-L or TRS-B, that the sequence of a TRS is directly responsible for regulating sgRNA levels, as also previously suggested (20) (Fig. 5). Recombinant virus BeauR-IR-CTGAACAA, with the introduction of a complete TRS-B for the IR matching the IBV S and gene 3 TRS-Bs of CUGAACAA, resulted in an increase in IR sgRNA levels to levels more consistent with those of upstream and downstream genes. In contrast, rIBV BeauR-L-CTTAACAT showed a decrease in IR sgRNA levels as a result of possessing only two nucleotide matches between the TRS-L and TRS-B at positions 6 and 7. The fact that IR sgRNAs could still be detected by standard and real-time PCR with only two matching nucleotides further strengthens the argument that homology in flanking sequences is required for recognition of a TRS-B and the subsequent pause/stop of the replication complex. Analysis of the sgRNA species produced by the TRS-L mutants did not reveal the presence of additional sgRNAs generated by activation of cryptic TRS sites, as has been observed previously (31, 33). This was particularly interesting to note during the analysis of rIBV BeauR-L-CTTAACAT. Although an exact CUUAACA sequence is found in the Beau-R genome beginning at nucleotide 24685, within the M gene, no sgRNA was transcribed via this potential TRS, demonstrating, as has been shown previously (23), that the conserved TRS is not sufficient for sgRNA synthesis. Further work is needed to investigate the effects of increasing/decreasing the homology of 5' and 3' flanking sequences for IBV TRSs and to establish which nucleotides are essential for optimal TRS recognition and template switching.

Northern blot analysis of rIBV BeauR $\Delta$ IR also revealed the presence of an additional RNA species slightly smaller than the S

sgmRNA and indicated by an asterisk in Fig. 1C. Investigation of this RNA revealed that it, too, was an sgmRNA with a leader-body junction of CUUAACAA and a noncanonical TRS-B, in this instance encompassing nucleotides 4 to 8, AACAA, of the consensus IBV TRS. This additional sgmRNA has a potential ORF in frame with the S gene sequence and encompassing amino acids 321 to 1162 of the full-length protein. However, it was not possible to detect this sgmRNA from any IBV strains other than Beau-R and the parent virus Beau-CK, suggesting that it is an artifact of the repeated passage of Beaudette on CK cells to generate the Beau-CK virus. It is unclear if this sgmRNA has any function during Beau-R/Beau-CK infection, but its presence provides evidence that the use of noncanonical TRS-Bs, in the form of shortened TRSs, may be more prevalent than suspected. A similar, truncated S protein has previously been reported for severe acute respiratory syndrome (SARS)-CoV that could be translated from a novel sgmRNA also generated via a noncanonical TRS (35).

Recombinant IBV BeauR-IR-CTGAACAA was not able to replicate to the peak levels observed for parental virus Beau-R in cell culture (Fig. 4A). The amino acid changes that arose within the M protein as a result of the point mutations introduced to create the CUGAACAA TRS-B are proposed as the reason for this. We suggest that the IR TRS-B could be viewed in terms of a series of point mutations that have arisen within the IR TRS-B in order to evolve a more viable M protein, thus resulting in a virus with improved replication. While the extended TRS-B was maintained by the virus, by passage 8 additional nucleotide mutations had arisen that resulted in a further amino acid change of A189T, suggesting the acquisition of compensatory mutations to counteract the loss of viability of M.

An alternative explanation for the nature of the IR TRS-B is that the noncanonical, truncated TRS-B has evolved to control the expression of the potential 11-kDa ORF protein through the generation of a low-abundance sgmRNA. Coronaviruses and, indeed, all viruses belonging to the *Nidovirales* order have evolved an extensive range of mechanisms for controlling expression of their genes. These include  $-1$  frameshifting to control the expression levels of the replicase proteins and the generation of a nested set of sgmRNAs for the expression of structural and accessory proteins, some of which require translation via leaky scanning or use of internal ribosome entry sequences.

The presence of natural deletions or truncations within the 11-kDa ORF gene of some IBV strains suggests a nonessential accessory role for the proposed protein. Previous work has shown that the IBV accessory proteins produced by genes 3 and 5 and accessory proteins of other coronaviruses can be deleted with no major impact on virus replication in cell culture (41–44). Here, we replaced the truncated 11-kDa ORF of Beau-R with eGFP and showed that the resultant rIBV expressed eGFP in cell culture (Fig. 3B). This demonstrated the translation of a protein from the IR sgmRNA and implies the expression of a fifth accessory protein by IBV. Attempts to identify the 11-kDa protein in cell culture using antibodies raised against the IBV M41 IR sequence have been unsuccessful.

In conclusion, in this study we have demonstrated the link between a previously uncharacterized RNA species of IBV and an ORF located between the M gene and gene 5. The identification and confirmation of a new sgmRNA for IBV and TCoV, transcribed via a noncanonical, shortened version of the consensus IBV/TCov TRS-B, has revealed the possibility that template

switching can occur within the conserved TRS-L in the absence of a full-length complementary TRS-B. The use of noncanonical TRS-Bs for synthesis of sgmRNAs may offer a potential mechanism by which coronaviruses can expand their repertoire of proteins. We propose that the IR sgmRNA is the template for the translation of a novel 11-kDa accessory protein of IBV and closely related gammacoronaviruses, bringing the total number of group-specific accessory proteins to five. It now remains important to identify this protein and establish its role in gammacoronavirus infection.

## ACKNOWLEDGMENTS

K. Bentley was the holder of a Biotechnology and Biological Sciences Research Council (BBSRC) Doctoral Training Grant Studentship. The work was supported by the BBSRC.

We are grateful to Nicolas Eterradossi and Olivier Guionie, French Agency for Food, Environmental and Occupational Health Safety, Ploufragan-Plouzane Laboratory, France, for providing turkey coronavirus RNA samples and to Richard C. Jones, Department of Veterinary Pathology, University of Liverpool, United Kingdom, for providing IBV strains CR88, D1466, H120, Italy-02, and QX used in this study. We also thank Helena Maier for providing TaqMan reagents.

## REFERENCES

- Cavanagh D. 2005. Coronaviruses in poultry and other birds. *Avian Pathol.* 34:439–448.
- Cavanagh D, Gelb J, Jr. 2008. Infectious bronchitis, p 117–135. *In* Saif YM, Fadly AM, Glisson JR, McDougald LR, Nolan LK, Swayne DE (ed), *Diseases of poultry*, 12th ed. Blackwell Publishing, Ames, IA.
- Jones RC. 2010. Viral respiratory diseases (ILT, aMPV infections, IB): are they ever under control? *Br. Poult. Sci.* 51:1–11.
- Sjaak de Wit JJ, Cook JKA, van der Heijden HMJF. 2011. Infectious bronchitis virus variants: a review of the history, current situation and control measures. *Avian Pathol.* 40:223–235.
- Britton P, Cavanagh D. 2007. Avian coronavirus diseases and infectious bronchitis vaccine development, p 161–181. *In* Thiel V (ed), *Coronaviruses: molecular and cellular biology*. Caister Academic Press, Norfolk, United Kingdom.
- Cook JKA, Mockett APA. 1995. Epidemiology of infectious bronchitis virus, p 317–335. *In* Siddell SG (ed), *The Coronaviridae*. Plenum Press, New York, NY.
- Cavanagh D. 2007. Coronavirus avian infectious bronchitis virus. *Vet. Res.* 38:281–297.
- Lambrechts C, Pensaert M, Ducatelle R. 1993. Challenge experiments to evaluate cross-protection induced at the trachea and kidney level by vaccine strains and Belgian nephropathogenic isolates of avian infectious bronchitis virus. *Avian Pathol.* 22:577–590.
- Ziegler AF, Ladman BS, Dunn PA, Schneider A, Davison S, Miller PG, Lu H, Weinstock D, Salem M, Eckroade RJ, Gelb J. 2002. Nephropathogenic infectious bronchitis in Pennsylvania chickens 1997–2000. *Avian Dis.* 46:847–858.
- Armesto M, Cavanagh D, Britton P. 2009. The replicase gene of avian coronavirus infectious bronchitis virus is a determinant of pathogenicity. *PLoS One* 4:e7384. doi:10.1371/journal.pone.0007384.
- Cao J, Wu CC, Lin TL. 2008. Complete nucleotide sequence of polyprotein gene 1 and genome organization of turkey coronavirus. *Virus Res.* 136:43–49.
- Hewson KA, Ignjatovic J, Browning GF, Devlin JM, Noormohammadi AH. 2011. Infectious bronchitis viruses with naturally occurring genomic rearrangement and gene deletion. *Arch. Virol.* 156:245–252.
- Gomaa MH, Barta JR, Ojckic D, Yoo D. 2008. Complete genomic sequence of turkey coronavirus. *Virus Res.* 135:237–246.
- Sawicki SG, Sawicki DL. 1995. Coronaviruses use discontinuous extension for synthesis of subgenome-length negative strands. *Adv. Exp. Med. Biol.* 380:499–506.
- Pasternak AO, Spaan WJ, Snijder EJ. 2006. Nidovirus transcription: how to make sense? *J. Gen. Virol.* 87:1403–1421.
- Sawicki SG, Sawicki DL, Siddell SG. 2007. A contemporary view of coronavirus transcription. *J. Virol.* 81:20–29.



17. Sola I, Mateos-Gomez PA, Almazan F, Zuniga S, Enjuanes L. 2011. RNA-RNA and RNA-protein interactions in coronavirus replication and transcription. *RNA Biol.* 8:237–248.
18. Pasternak AO, van den Born E, Spaan WJ, Snijder EJ. 2001. Sequence requirements for RNA strand transfer during nidovirus discontinuous subgenomic RNA synthesis. *EMBO J.* 20:7220–7228.
19. van Marle G, Dobbe JC, Gulyaev AP, Luytjes W, Spaan WJ, Snijder EJ. 1999. Arterivirus discontinuous mRNA transcription is guided by base pairing between sense and antisense transcription-regulating sequences. *Proc. Natl. Acad. Sci. U. S. A.* 96:12056–12061.
20. Zuniga S, Sola I, Alonso S, Enjuanes L. 2004. Sequence motifs involved in the regulation of discontinuous coronavirus subgenomic RNA synthesis. *J. Virol.* 78:980–994.
21. Dufour D, Mateos-Gomez PA, Enjuanes L, Gallego J, Sola I. 2011. Structure and functional relevance of a transcription-regulating sequence involved in coronavirus discontinuous RNA synthesis. *J. Virol.* 85:4963–4973.
22. Moreno JL, Zuniga S, Enjuanes L, Sola I. 2008. Identification of a coronavirus transcription enhancer. *J. Virol.* 82:3882–3893.
23. Ozdarendeli A, Ku S, Rochat S, Williams GD, Senanayake SD, Brian DA. 2001. Downstream sequences influence the choice between a naturally occurring noncanonical and closely positioned upstream canonical heptameric fusion motif during bovine coronavirus subgenomic mRNA synthesis. *J. Virol.* 75:7362–7374.
24. Yang D, Liu P, Giedroc DP, Leibowitz J. 2011. Mouse hepatitis virus stem-loop 4 functions as a spacer element required to drive subgenomic RNA synthesis. *J. Virol.* 85:9199–9209.
25. Hiscox JA, Mawditt KL, Cavanagh D, Britton P. 1995. Investigation of the control of coronavirus subgenomic mRNA transcription by using T7-generated negative-sense RNA transcripts. *J. Virol.* 69:6219–6227.
26. Sola I, Moreno JL, Zuniga S, Alonso S, Enjuanes L. 2005. Role of nucleotides immediately flanking the transcription-regulating sequence core in coronavirus subgenomic mRNA synthesis. *J. Virol.* 79:2506–2516.
27. Stern DF, Kennedy SI. 1980. Coronavirus multiplication strategy. I. Identification and characterization of virus-specified RNA. *J. Virol.* 34:665–674.
28. Casais R, Thiel V, Siddell SG, Cavanagh D, Britton P. 2001. Reverse genetics system for the avian coronavirus infectious bronchitis virus. *J. Virol.* 75:12359–12369.
29. Britton P, Evans S, Dove B, Davies M, Casais R, Cavanagh D. 2005. Generation of a recombinant avian coronavirus infectious bronchitis virus using transient dominant selection. *J. Virol. Methods* 123:203–211.
30. Armesto M, Casais R, Cavanagh D, Britton P. 2008. Transient dominant selection for the modification and generation of recombinant infectious bronchitis coronaviruses. *Methods Mol. Biol.* 454:255–273.
31. Yount B, Roberts RS, Lindesmith L, Baric RS. 2006. Rewiring the severe acute respiratory syndrome coronavirus (SARS-CoV) transcription circuit: engineering a recombination-resistant genome. *Proc. Natl. Acad. Sci. U. S. A.* 103:12546–12551.
32. Schaad MC, Baric RS. 1994. Genetics of mouse hepatitis virus transcription: evidence that subgenomic negative strands are functional templates. *J. Virol.* 68:8169–8179.
33. Pasternak AO, van den Born E, Spaan WJ, Snijder EJ. 2003. The stability of the duplex between sense and antisense transcription-regulating sequences is a crucial factor in arterivirus subgenomic mRNA synthesis. *J. Virol.* 77:1175–1183.
34. Zhang X, Liu R. 2000. Identification of a noncanonical signal for transcription of a novel subgenomic mRNA of mouse hepatitis virus: implication for the mechanism of coronavirus RNA transcription. *Virology* 278:75–85.
35. Hussain S, Pan J, Chen Y, Yang Y, Xu J, Peng Y, Wu Y, Li Z, Zhu Y, Tien P, Guo D. 2005. Identification of novel subgenomic RNAs and noncanonical transcription initiation signals of severe acute respiratory syndrome coronavirus. *J. Virol.* 79:5288–5295.
36. Mateos-Gomez PA, Zuniga S, Palacio L, Enjuanes L, Sola I. 2011. Gene N proximal and distal RNA motifs regulate coronavirus nucleocapsid mRNA transcription. *J. Virol.* 85:8968–8980.
37. Baric RS, Nelson GW, Fleming JO, Deans RJ, Keck JG, Casteel N, Stohlman SA. 1988. Interactions between coronavirus nucleocapsid protein and viral RNAs: implications for viral transcription. *J. Virol.* 62:4280–4287.
38. Zhang X, Lai MM. 1995. Interactions between the cytoplasmic proteins and the intergenic (promoter) sequence of mouse hepatitis virus RNA: correlation with the amounts of subgenomic mRNA transcribed. *J. Virol.* 69:1637–1644.
39. Zuniga S, Cruz JL, Sola I, Mateos-Gomez PA, Palacio L, Enjuanes L. 2010. Coronavirus nucleocapsid protein facilitates template switching and is required for efficient transcription. *J. Virol.* 84:2169–2175.
40. Keane SC, Liu P, Leibowitz JL, Giedroc DP. 2012. Functional transcriptional regulatory sequence (TRS) RNA binding and helix destabilizing determinants of murine hepatitis virus (MHV) nucleocapsid (N) protein. *J. Biol. Chem.* 287:7063–7073.
41. Casais R, Davies M, Cavanagh D, Britton P. 2005. Gene 5 of the avian coronavirus infectious bronchitis virus is not essential for replication. *J. Virol.* 79:8065–8078.
42. de Haan CA, Masters PS, Shen X, Weiss S, Rottier PJ. 2002. The group-specific murine coronavirus genes are not essential, but their deletion, by reverse genetics, is attenuating in the natural host. *Virology* 296:177–189.
43. Hodgson T, Britton P, Cavanagh D. 2006. Neither the RNA nor the proteins of open reading frames 3a and 3b of the coronavirus infectious bronchitis virus are essential for replication. *J. Virol.* 80:296–305.
44. Yount B, Roberts RS, Sims AC, Deming D, Frieman MB, Sparks J, Denison MR, Davis N, Baric RS. 2005. Severe acute respiratory syndrome coronavirus group-specific open reading frames encode nonessential functions for replication in cell cultures and mice. *J. Virol.* 79:14909–14922.